Organic & Biomolecular Chemistry

PAPER

View Article Online
View Journal | View Issue

Cite this: *Org. Biomol. Chem.*, 2014, **12**, 2606

Versatile C_3-symmetric scaffolds and their use for covalent stabilization of the foldon trimer†

Arne Berthelmann,[a] Johannes Lach,[a] Melissa A. Gräwert,[b,c] Michael Groll[b] and Jutta Eichler*[a]

Received 12th November 2013,
Accepted 18th February 2014

DOI: 10.1039/c3ob42251h

www.rsc.org/obc

C_3-Symmetric trimesic acid scaffolds, functionalized with bromoacetyl, aminooxyacetyl and azidoacetyl moieties, respectively, were synthesized and compared regarding their utility for the trivalent presentation of peptides using three different chemoselective ligation reactions, *i.e.* thioether and oxime formation, as well as the "click" reaction. The latter ligation method was then used to covalently stabilize the trimer of foldon, a 27 amino acid trimerization domain of bacteriophage T4 fibritin, by linking the three foldon monomers to the triazido-functionalized trimesic acid scaffold. This reaction dramatically enhanced the thermal stability of the trimer, while maintaining the correct fold, as demonstrated by CD spectroscopy and X-ray crystal structure analysis, respectively, of the foldon–scaffold conjugates.

Introduction

Multivalent interactions play an important role in biological systems,[1] as exemplified by receptor oligomers.[2] Trimeric ligands, such as the tumor necrosis factor (TNF) superfamily,[3] are often presented in the shape of C_3-symmetric molecules. C_3-Symmetric trimeric proteins are also involved in the complex interplay between pathogens, such as the human immunodeficiency virus (HIV-1), and their host cells.[4] Interactions of the HIV-1 envelope protein (Env), which is presented as a C_3-symmetric trimer on the virus surface,[5] with cellular receptors are involved in a cascade of binding events that result in virus entry into the cell.[6] Synthetic peptides have proven excellent molecular tools to explore the chemical and structural determinants of protein–protein interactions.[7] Accordingly, peptides to be used for studying molecular interactions involving trimeric proteins should also be presented as trimers, which requires ready and fast synthetic access to such trivalent peptides. Addressing this challenge, we have synthesized three differently functionalized trivalent C_3-symmetric scaffolds to which peptides can be covalently linked *via* different chemoselective ligation strategies. For this, we explored three different ligation reactions: thioether formation from an α-haloalkyl and a thiol group,[8] the generation of 1,2,3-triazoles through 1,3-dipolar cycloaddition of an azide to an alkyne,[9] as well as oxime formation from an aldehyde and a hydroxylamine.[10]

Typically, the purpose of multivalent presentation is to bring into spatial proximity molecules that normally would not self-associate into an oligomer. An alternative strategy is covalent linkage of monomers of a pre-organized oligomer. Such covalently stabilized oligomers could be useful in experiments involving low, *i.e.* nano- and picomolar concentrations, where the native, non-covalent oligomer may no longer be sufficiently stable. Such a beneficial effect of covalent stabilization has been shown for peptides that present parts of the N-peptide region of HIV-1 gp41 fused to a trimeric coiled coil.[11] Covalent stabilization of this trimer by introducing multiple inter-chain disulfide bridges dramatically enhanced the HIV-1 inhibitory activity of these trimeric peptides, most likely due to increased thermodynamic stability of the trimer.[12]

The C-terminal domain of fibritin, a structural protein of bacteriophage T4, has been shown to be essential for fibritin trimerization and folding.[13] This domain, termed foldon, assembles into a β-propeller-like trimeric structure in which each subunit consists of a single β-hairpin.[14] Using a peptide presenting only the 27 amino acid foldon sequence, this characteristic fold has been shown to be independent of the structural context of the fibritin protein.[15] Furthermore, the trimeric structure of the foldon is largely unaffected by

[a]*Department of Chemistry and Pharmacy, University of Erlangen-Nurnberg, Schuhstr. 19, 91052 Erlangen, Germany. E-mail: jutta.eichler@fau.de; Fax: +49-9131-852-2587; Tel: +49-9131-852-4117*

[b]*Center for Integrated Protein Science at the Department of Chemistry, Chair of Biochemistry, Technical University of Munich, Lichtenbergstr. 4, 85747 Munich, Germany. E-mail: michael.groll@ch.tum.de; Fax: +49-89-289-13363; Tel: +49-89-289-13361*

[c]*European Molecular Biology Laboratory, Hamburg Unit, EMBL c/o DESY, Notkestraße 85, 22603 Hamburg, Germany. E-mail: graewert@embl-hamburg.de; Fax: +49-40-89902-149; Tel: +49-40-89902-115*

†Electronic supplementary information (ESI) available: NMR spectra of **3** through **8**; LC-MS data/MALDI spectra of **9** through **17**; X-ray data collection and refinement statistics of foldon–scaffold conjugates; thermal unfolding of the non-covalent foldon trimer (**15**), as well as the covalently stabilized trimers **18** and **19**, in a buffer without detergent. See DOI: 10.1039/c3ob42251h

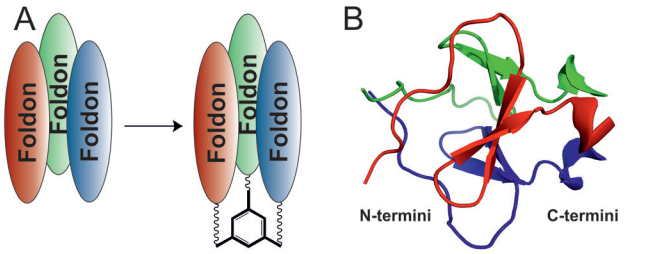

Fig. 1 (A) Covalent stabilization of the foldon trimer by N- or C-terminally linking the three monomers to a C_3-symmetric scaffold. (B) Location of N-and C-termini, respectively, of the three monomers within the foldon NMR structure (PDB ID: 1RFO).[15]

proteins attached to it, rendering this domain an ideal auxilliary to induce or stabilize trimeric structures of peptides and proteins. Examples of such foldon fusion proteins include HIV-1 gp41,[16] a tumor necrosis factor ligand,[17] as well as a recombinant influenza H5N1 vaccine.[18]

Here, we asked whether the thermodynamic stability of the foldon trimer could be enhanced, while maintaining the correct fold, by covalently linking the three monomers to a C_3-symmetric scaffold (Fig. 1).

Results and discussion

Synthesis of scaffolds

Benzene-1,3,5-tricarboxylic acid (trimesic acid) **1**, containing a 3-fold axis, served as a starting point for the generation of the different scaffolds. The utility of this simple aromatic compound for the synthesis of complex trimeric structures, such as monodisperse dendrimers,[19] symmetric LewisX antigens[20] or trimeric integrin ligands,[21] has been demonstrated before.

In order to provide a trivalent amino-functionalized scaffold, N^1-Boc-3,6-dioxaoctane-1,8-diamine (Boc-DOOA) **2** was coupled as a spacer to the three carboxylic groups of **1** using 1-ethyl-3-(3-dimethylaminopropyl)carbodiimide (EDCI) as a coupling reagent, yielding the Boc-protected scaffold **3** (Scheme 1, Fig. S1 and S2†). EDCI was chosen because it facilitates work-up of the product through simple aqueous extraction of the resulting water-soluble urea derivative.[22] Removal of the Boc groups yielded the C_3-symmetric scaffold **4** (Scheme 1, Fig. S3 and S4†). The ethylene glycol nature of the diamine spacer **2** was chosen based on its favorable chemical and physical characteristics, which include solubility in

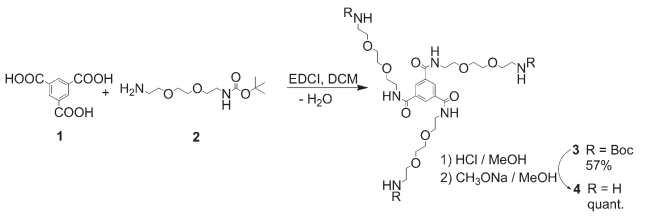

Scheme 1 Synthesis of the amino-functionalized trimesic acid scaffold **4**.

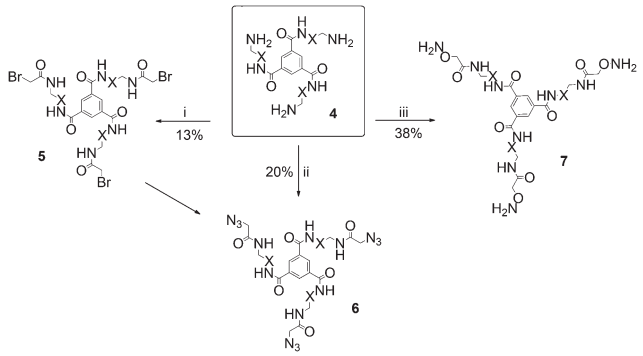

Scheme 2 Functionalization of the amino scaffold **4** for different ligation reactions. (i) Bromoacetic acid/DIC; (ii) azidoacetic acid/EDCI; (iii) (a) AOA/EDCI, (b) TFA/DCM; X: $-(CH_2)_2-O-(CH_2)_2-O-(CH_2)_2-$.

organic solvents, such as dichloromethane or chloroform, in which scaffold synthesis was carried out, as well as in aqueous media for the subsequent ligation reaction with peptides. Furthermore, PEG based spacers are flexible, non-toxic and non-immunogenic.[23]

Scaffold **4** provided the basis for the generation of three differently functionalized trimeric scaffolds, through acylation with different acetic acid derivatives (Scheme 2). The bromoacetylated scaffold **5**, which served as a precursor for subsequent thioether ligation, was synthesized by acylating the amino groups of **4** with bromoacetic acid. For this reaction, EDCI turned out to be a poor coupling reagent, since it was used as a hydrochloride, resulting in a halide exchange of the bromo alkyl group, yielding the less reactive chloroacetyl scaffold derivative. This reaction could be avoided by using *N*,*N*′-diisopropylcarbodiimide (DIC) as the coupling reagent, which yielded the desired bromoacetyl scaffold derivative **5** (Fig. S5 and S6†).

The triazido scaffold **6** was generated by two different approaches. The first strategy involved coupling of pre-formed azidoacetic acid **8**[24] (Fig. S11 and S12†) in conjunction with EDCI to yield **6** (20% isolated). The second method was based on a pseudo halide exchange of the haloacetylated scaffold **5** with sodium azide in the presence of 18-crown-6-ether.[25] Both methods worked equally well, yielding **6** as the desired product (Fig. S7 and S8†).

The hydroxylamine functionality required for subsequent oxime ligation was introduced by coupling bis-Boc protected (aminooxy)acetic acid (AOA) to the triamino scaffold **4**, followed by removal of the Boc groups with trifluoroacetic acid (TFA), yielding tris(aminooxy)-functionalized scaffold **7** quantitatively (Fig. S9 and S10†).

Ligation reactions

The utility of the three differently functionalized scaffolds **5**, **6** and **7** for the respective ligation reactions was tested using the peptide sequence AKYRP, a short trypsin inhibitor.[26] This peptide was synthesized thrice (peptides **9**, **10** and **11**). The sequence was N-terminally extended by ε-aminohexanoic acid

(Ahx) as a spacer, followed by an N-acetylated cysteine (peptide **9**, Fig. S13†), N-acetylated propargyl glycine (peptide **10**, Fig. S14†), and 4-formylbenzoic acid (peptide **11**, Fig. S15†), respectively. For the cleavage of peptide **11** from the resin, the scavenger composition of the TFA cocktail had to be modified in order to avoid side reactions, in particular reduction of the aldehyde to the alcohol. Therefore, thioanisole was omitted from the cleavage cocktail, and formylbenzoic acid was added as an additional scavenger. All three peptides could be synthesized in good yields of 42–58%.

The functionalized scaffolds **5**, **6** and **7**, as well as peptides **9**, **10** and **11**, subsequently served as mutually reactive precursors for the three ligation reactions to be studied (Scheme 3). To analyze and compare the kinetics of these ligations, the reaction progress was followed by LC-MS over time.

Formation of a thioether from haloacetylated and thiol containing precursors in aqueous media (Scheme 3A) is well established.[27] This reaction, however, is not absolutely chemoselective. Peptide dimerization through disulfide formation is a prominent side reaction, which can be reversed by reducing the disulfide using tris(2-carboxyethyl)phosphine (TCEP).[28] The ligation reaction was performed at pH 9.6 to provide a highly nucleophilic thiolate species of **9**. As shown in Fig. 2A, the trimeric product **12** (Fig. S16†) was generated instantaneously upon mixing of precursors **5** and **9**. The first LC-MS sample was taken after approximately 1 min at which time the conversion rate was already 55%, indicating a very fast reaction. Kinetic analysis by HPLC indicated 85% conversion to the thioether trimer within 30 min. The disulfide dimer of **9** was detected merely as a minor side product, while the remaining side products were identified as mono- and di-substituted scaffolds, respectively. These results demonstrate that thioether ligation is an excellent method for the generation of trivalent peptides. Furthermore, this method can also be used to trimerize proteins using free cysteine residues in their sequences as ligation points.

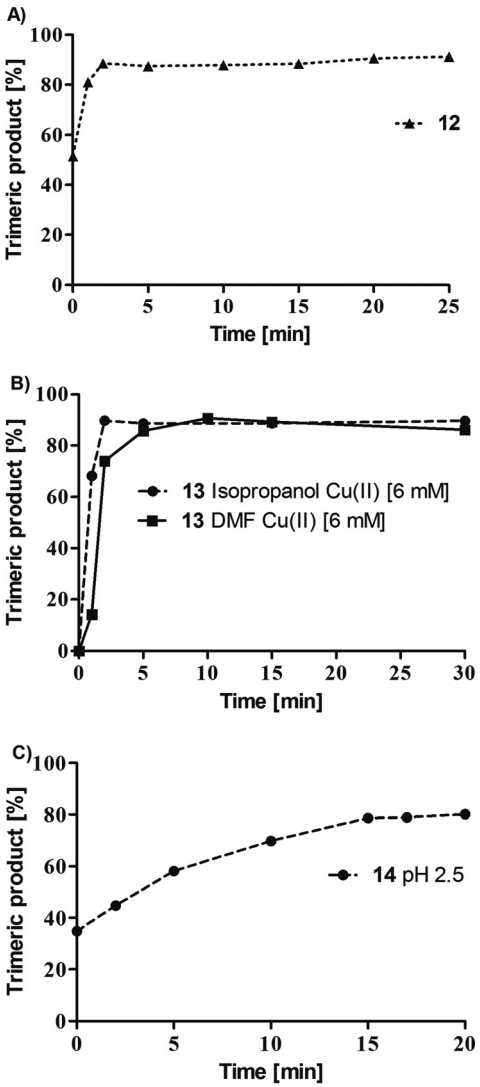

Fig. 2 Kinetics of ligation reactions: (A) thioether ligation (generation of **12**), (B) 1,3-dipolar cycloaddition (generation of **13**), (C) oxime ligation (generation of **14**). Monomeric peptides were used at 3 mM and scaffolds at 1 mM, resulting in a concentration of 1 mM for the generated trivalent peptides.

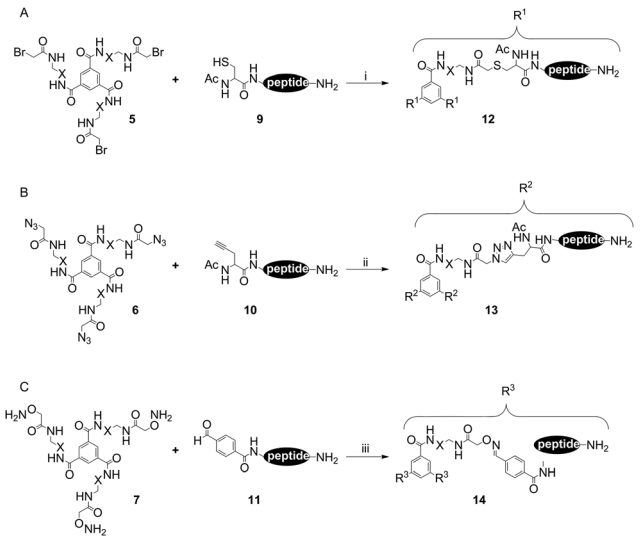

Scheme 3 Ligation reactions. (A) Thioether ligation; (B) 1,3-dipolar cycloaddition; (C) oxime ligation. (i) Carbonate buffer pH 9.6; (ii) 6 M $CuSO_4$, 18 M sodium ascorbate; (iii) citrate buffer pH 2.5. X: $-(CH_2)_2-O-(CH_2)_2-O-(CH_2)_2-$; peptide: Ahx-AKIYRP.

Copper(I)-catalyzed 1,3-dipolar cycloaddition of azides to alkynes generates 1,4-substituted (1,2,3)-triazoles (Scheme 3B) and is better known as "click chemistry".[29] This type of chemoselective reaction has been extensively used to generate diverse bioactive molecules, including combinatorial peptidotriazole libraries,[30] cyclopeptide analogs,[31] or β-turn mimics.[32] The click reaction is controlled by several parameters, most importantly the source of Cu(I). A convenient way to provide the catalytic Cu(I) species is *in situ* reduction of Cu(II)-salts with a suitable reductive agent, such as ascorbic acid. Another critical factor is the solvent. While an aqueous environment is favorable for reactions involving unprotected peptides, protected or

resin-bound peptides, as well as other, less polar compounds, require a polar organic solvent. To cover both scenarios, two solvent mixtures were tested, *i.e.* a water–isopropanol (1 : 1) and a water–DMF (1 : 1) mixture.

Similar to the thioether ligation, kinetic analysis (Fig. 2B) demonstrated a fast reaction of peptide **10** with triazido scaffold **6**. In isopropanol, the reaction was almost complete within 10 min, with a conversion rate to the trimeric product **13** (Fig. S17†) of 86% (isopropanol) and 90% (DMF), respectively, illustrating the outstanding value of click chemistry for the chemoselective attachment of alkyne peptides to C_3-symmetric azido scaffolds. Mono- and disubstituted scaffolds were found as side products (11% and 9%, respectively), whereas only traces of unreacted **10** were detectable after 30 minutes.

Finally, oxime ligation[33] was used to generate trivalent peptide **14** by reacting the nucleophilic hydroxylamines of scaffold **7** with peptide **11**, which was N-terminally acylated with 4-formylbenzoic acid, providing the aldehyde moiety for oxime formation (Scheme 3C). Analysis of reaction kinetics for the formation of **14** (Fig. S18†) indicated a maximal yield of 80% after 20 minutes (Fig. 2C), which could not be further improved over time. As expected,[34] addition of aniline as a catalyst accelerated the reaction, but did not improve the final yield (data not shown). Interestingly, the main side product here was unreacted **11** (18%) rather than the respective mono- and disubstituted scaffolds. It should also be noted that the trimerization yields of parallel experiments involving an analog of **11**, in which the aldehyde moiety was replaced by a ketone (pyruvoyl moiety), were much lower and did not exceed 23% after 10 hours.

Comparing the results of the above three ligation strategies, it is apparent that thioether ligation and click reaction yielded the desired trivalent peptides in excellent yields and purities, while the results of the oxime ligation were less satisfactory. Furthermore, all three methods have their specific strengths and limitations. Thioether ligation yields metabolically stable and largely non-reactive molecules that are well compatible with biological systems. In fact, methionine, one of the proteinogenic amino acids, contains a thioether in its side chain. Possible side reactions associated with thioether ligation include an attack of other nucleophilic moieties on the bromoacetylated scaffold, impairing the site-selectivity of the ligation reaction. Similarly, the carbonyl carbon of the aldehyde or ketone moieties involved in oxime ligation may also be attacked by nucleophiles other than the cognate aminooxy group of the scaffold. Furthermore, the limited choice of scavengers to be used during the acidic cleavage of the aldehyde peptide precursor from the resin may impair the purity of longer peptides containing multiple side chain protection groups. In addition, due to the susceptibility of oximes to hydrolysis, this ligation reaction may not be ideal for the generation of molecules to be used in biological systems. Triazoles, on the other hand, which are the product of the click reaction, are thought to be fairly stable in a range of different milieus. It should be noted, however, that the nitrogen atoms of the triazole ring are potentially strong hydrogen bond acceptors in biomolecular interactions, which may mask the native interactions. These specifics should be taken into account when selecting a ligation strategy for a specific application.

Covalent stabilization of the foldon trimer

Based on the excellent results obtained using the click reaction to attach peptide monomers to the trimesic acid scaffold, as well as the robustness of this reaction and ease of synthesis of precursors, we chose the click reaction to covalently stabilize the trimer of the 27 amino acid peptide foldon. The three dioxaoctane spacer units of scaffold **6** were thought to be adequate to cover the distances between the N-(13.7 Å) and C- (5.15 Å) termini of the three foldon monomers within the trimer structure. In addition to the unmodified foldon sequence (**15**, Fig. S19†), we synthesized two peptides, in which a propargylglycine residue was added either to the N- or C-terminus of the foldon sequence (**16** and **17**, Fig. S20 and S21,† see Table 1 for peptide sequences). These functionalized peptides were then "clicked" to the triazido scaffold **6**, yielding conjugates **18** and **19** (Fig. 3 and S22 through S25†), whose folding and thermal stabilities were subsequently analyzed by CD spectroscopy and X-ray crystal structure analysis, respectively.

Comparison of the CD spectra of **15**, **18** and **19** indicated that covalent attachment of the three foldon monomers to the scaffold does not affect folding of the trimer, as all three CD spectra are very similar (Fig. 4).

The notion of structural similarity between wt foldon (**15**) and the two foldon–scaffold conjugates was corroborated by

Table 1 Peptide sequences

Peptide	Sequence
9	Ac-CX[a]AKIYRP-NH_2
10	Ac-Pra[b]-XAKIYRP-NH_2
11	Fba[c]-XAKIYRP-NH_2
15	Ac-GYIPEAPRDGQAYVRKDGEWVLLSTFL-NH_2
16	Ac-Pra-XGYIPEAPRDGQAYVRKDGEWVLLSTFL-NH_2
17	Ac-GYIPEAPRDGQAYVRKDGEWVLLSTFLX-Pra-NH_2

[a] X, 6-aminohexanoic acid. [b] Pra, propargylglycine. [c] Fba, 4-formylbenzoic acid; Ac, acetyl.

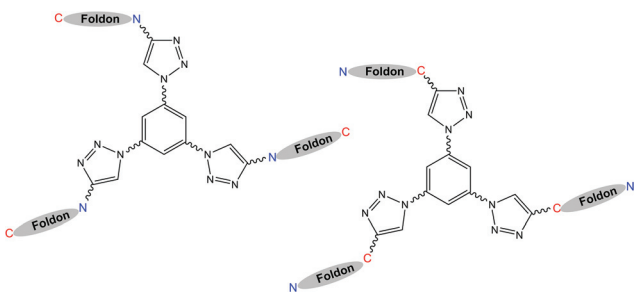

Fig. 3 Covalently stabilized foldon trimers, in which the three monomers are linked N- (**18**, left) and C- (**19**, right) terminally respectively, *via* triazole linkers, to a trimesic acid scaffold.

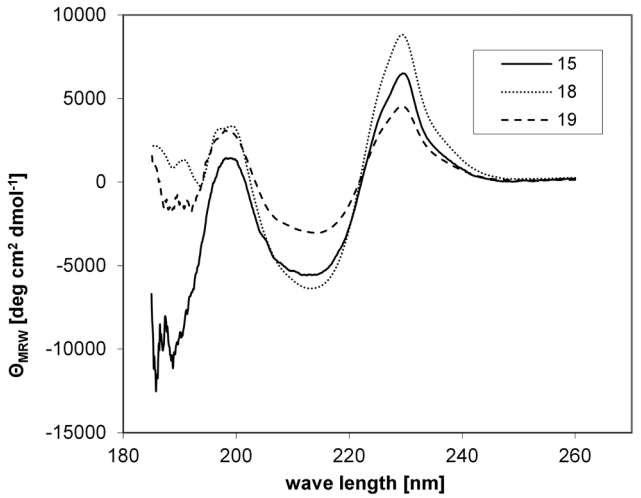

Fig. 4 CD spectra of the non-covalent foldon trimer (**15**), as well as covalently stabilized trimers **18** and **19**.

solving the crystal structures of **18** and **19**, and comparing it with the structure of wt foldon. Conjugates **18** and **19** were subjected to a number of crystallization trials with various salts at different concentrations. The conjugates spontaneously crystallized in more than 70% of the tested buffers (approximately 500). The most promising crystals were obtained in 0.2 M ammonium sulfate, 30% PEG 4000 and 1.4 M Na/K-phosphate, pH 5. Despite the relatively small size of the crystals, high resolution data could be collected up to 1.1 Å resolutions. Interestingly, the X-ray data revealed a high tendency of the foldon to crystallize in different space groups. Even crystals harvested from the same drop showed different symmetries. We determined the structures of conjugates **18** and **19**, which crystallized in the space groups $p2_1$ (1.1 Å) and $C2$ (1.3 Å). Both proteins present a native-like fold, comprising a 3_{10}-helix at the C-terminus, which is preceded by a β-hairpin and an extended structure at the N-terminus (Fig. 5). Superposition of **18** and **19** with wt foldon (PDB ID 4NCU) confirmed the overall similarity of the three structures, as local heterogeneity is only observed at the flexible spacer region (root mean square deviation of C_α < 0.3 Å) (Fig. 5a and S27†). Furthermore, the structures are largely congruent with the previously solved NMR structure.[15] The calculated size of the interface between the three foldon monomers (approximately 3000 Å^2) was very similar in wt foldon and the covalently stabilized trimers **18** and **19**. The scaffold and linker regions of **18** and **19**, however, are resolved differently in the two structures. The electron density map of **18** merely displays the amide part of the linker that is directly attached to the foldon N-terminus (Fig. 5b). In the structure of **19**, on the other hand, the trimesic acid scaffold is well defined and positioned at the center of the tri-fold non-crystallographic symmetry axis atop the C-terminal leucine residues, whereas the first three N-terminal foldon residues, as well as the linker region composed of 6-aminohexanoic acid, the triazole ring and DOOA, are structurally distorted (Fig. 5c). In summary, the crystallographic data confirm that the structure of the foldon trimer is largely unaffected by covalent linking of the three monomers to the trimesic acid scaffold.

Thermal unfolding of wt and covalently stabilized foldon trimers was assessed by monitoring the temperature-dependent changes in CD signals at 228 nm.[35]

As shown in Fig. 6, the stability of the trimer was greatly enhanced by covalently attaching the three monomers to the trimesic acid scaffold, as evidenced by a strong shift in T_m of **18** and **19**, compared to **15**. Even under denaturing conditions (5 M urea), the covalently stabilized trimers (**18**, T_m = 77 °C and **19**, T_m = 78 °C) were substantially more stable, with T_m approximately 30 degrees higher than that of the non-covalent foldon (**15**, T_m = 48 °C) (Fig. 6). In a buffer without detergent, on the other hand, the trimers of **18** and **19** did not start to unfold until temperatures as high as 80 °C were reached, so that no melting points could be determined (Fig. S26†). These results demonstrate a strong stabilization of the foldon trimer by covalently attaching the three monomers to a C_3-symmetric scaffold, regardless of the orientation of the foldon sequence with respect to the scaffold (N- and C-terminal attachment, respectively).

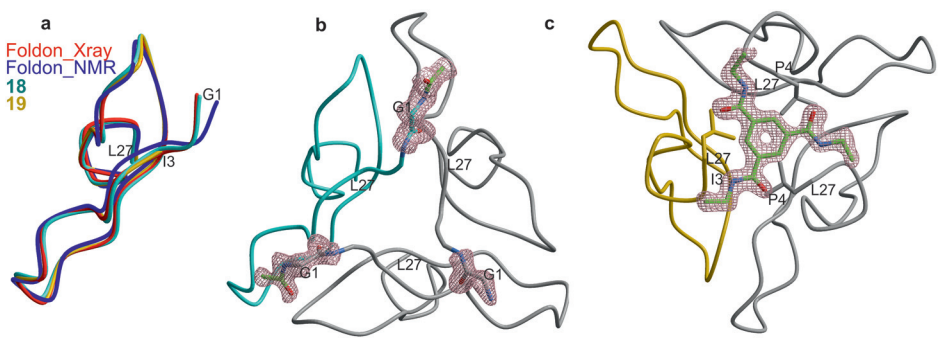

Fig. 5 (a) Backbone superposition of one monomer of wt foldon (red: crystal structure (PDB ID 4NCU), purple: NMR structure[15]) with the covalent conjugates **18** (cyan) and **19** (gold). The structurally distorted N-termini of **19** are labelled. (b) Trimer structure of **18**. The acetamide of the linker is well defined in the electron density map. (c) Trimer structure of **19** (rotated about the *x*-axis by 180°). The electron density (blue) represents a $2F_O$–F_C-omit map contoured at 1.0 σ of the trimesic acid scaffold.

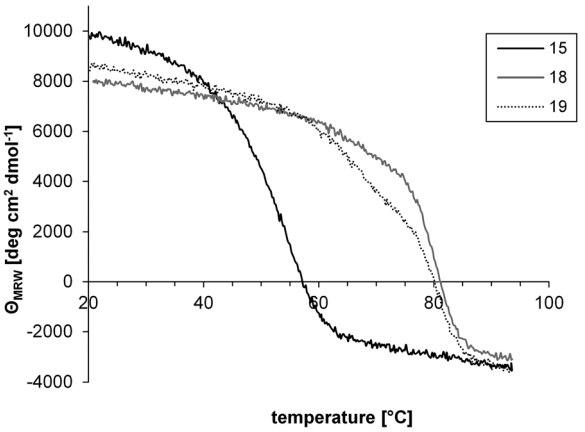

Fig. 6 Thermal unfolding of the non-covalent foldon trimer (**15**), as well as the covalently stabilized trimers **18** and **19**, in the presence of 5 M urea.

Experimental section

Materials and methods

Thin-layer chromatography. Thin-layer chromatography was performed on silica gel 60 F254 on aluminum foils (Merck). Compounds were detected under a UV lamp at 254 nm and 366 nm, respectively.

Column chromatography. Column chromatography was performed using Merck Silica Gel 60 (0.04–0.063 nm) as the stationary phase.

^{1}H/^{13}C-NMR spectra. ^{1}H/^{13}C-NMR spectra were recorded on Bruker Avance 600 (^{1}H: 600 MHz, ^{13}C: 151 MHz) and Bruker Avance 360 (^{1}H: 360 MHz, ^{13}C: 91 MHz) using $CDCl_3$, CD_3OD and CD_3CN as solvents referenced to TMS (0 ppm), $CHCl_3$ (7.26 ppm), CHD_2OD (3.31 ppm) or CHD_2CN (1.94 ppm). Chemical shifts are reported in parts per million (ppm). Coupling constants (J) are in hertz (Hz). The following abbreviations are used for the description of signals: s (singlet), d (doublet), t (triplet), q (quadruplet), m (multiplet).

LC-MS. Analytical HPLC was performed with online ESI mass spectrometry detection (LC-MS) using an Agilent HP 1100 instrument, and the following conditions: column: Kinetex C18, 2.6 μm, 100 Å, 50 × 2.1 mm, flow rate: 0.4 mL min^{-1}, gradient: 5–95% ACN–water (both containing 0.1% TFA) in 15 min. Mass spectra were measured on an AB SCIEX API 2000. The recorded spectra were analyzed using the Analyst software (1.4.2) by AB SCIEX.

Preparative HPLC. The following conditions were applied: column: Reprosil 100 C18, 5 μm, 250 × 10 mm, flow rate: 9 mL min^{-1}, gradient: 15–55% ACN–water (both containing 0.1% TFA) in 60 min (**12–14**), and 20–60% in 80 min (**15–19**), respectively, UV detection at 220 nm.

High resolution ESI mass spectrometry. High resolution ESI mass spectra were recorded on a Bruker Daltonik Maxis 4G using electrospray ionization in the positive mode. Peptides were dissolved in ACN–H_2O at 1 mg mL^{-1}. The recorded spectra were analysed using the open source mass spectrometry tool mMass.

Peptide synthesis. Peptides (see Table 1 for sequences) were synthesized as C-terminal amides by Fmoc/*t*-Bu-based solid-phase synthesis on 100 mg TentaGel S RAM resin (0.24 mmol g^{-1}) from Rapp Polymere, using an automated multiple peptide synthesizer (SYRO I from MultiSynTech). In a standard coupling cycle, five eq. of Fmoc-amino acid/DIC/HOBt in DMF were coupled for 60 min, followed by a capping step using a mixture of acetic anhydride–pyridine–DMF (1 : 2 : 3; 30 min). The Fmoc group was removed using 20% piperidine–DMF (20 min). Fmoc-propargyl glycine (peptides **10**, **16** and **17**) as well as 4-formylbenzoic acid (peptide **11**) were coupled overnight using 3 and 10 eq., respectively, of activated acid. To avoid aspartimide formation in peptides **15**, **16** and **17**, Fmoc-L-Asp(OMpe)-OH was used to introduce aspartic acid residues in these peptides. Peptide **9**, **10**, **15**, **16** and **17** were cleaved from the resin using a mixture of TFA–thioanisole–phenol–water–EDT (82.5 : 5 : 5 : 5 : 2.5). Peptide **11** was cleaved with a mixture of TFA–TIPS–4-formylbenzoic acid–water (85 : 5 : 5 : 5) to avoid reduction of the aldehyde group. The cleaved peptides were precipitated in a cold 1 : 1 mixture of cyclohexane and *t*-butyl methyl ether (10 mL), extracted with water (10 mL), lyophilized twice, purified by preparative HPLC, and characterized by LC-MS and high resolution ESI mass spectrometry, respectively.

CD spectra. CD spectra of **15**, **18** and **19** were recorded using a Jasco J-815 instrument at 20 °C and 50 μM in phosphate buffer pH 7.0. Thermal unfolding transitions were measured by monitoring the changes in CD signals at 228 nM at peptide concentrations of 30 μM (**18** and **19**) and 90 μM (**15**), respectively, in phosphate buffer pH 7.0, as well as in the same buffer containing 5 M urea.

Crystal structure analysis. The covalently stabilized folden trimers **18** and **19** were dissolved in water at 8–12 mg mL^{-1}. The initial crystallization conditions were determined by the sitting drop vapor diffusion method at 20 °C. For this, equal volumes (0.1 μL + 0.1 μL) of protein solution and precipitant solution were mixed (crystal screens ClassicsI, ClassicsII, JCSG, PEG I and PEG II suites (Qiagen, Hilden)) using the robot from Art Robbins (Phoenix), and equilibrated against the reservoir containing 45 μL crystallization solution. In general, crystal formation could be observed within a few hours. Suitable conditions were further optimized using the hanging drop vapor diffusion method, resulting in the selection of 20% PEG 200, 0.2 M ammonium sulfate, 30% PEG 4000 and 1.4 M Na/K-phosphate, pH 5. Crystals were soaked in cryobuffer containing 25% PEG 200 in addition to the precipitant solution, and cooled in a stream of nitrogen gas at 100 K (Oxford Cryo Streams). Datasets were collected using the synchrotron radiation facility at the X06SA-beamline, SLS (Villigen, Switzerland) (Table S1†). Datasets were processed either with PROTEUM2 or using the program package XDS.[36] For structure determination, molecular replacement was performed in PHASER[37] by using the coordinates of a wild type foldon structure solved by NMR spectroscopy (PDB ID: 1RFO). The models were completed using the interactive three-dimensional graphics program MAIN.[38] Conventional crystallographic rigid body,

positional, and temperature factor refinements were carried out with REFMAC5 from the CCP4 package.[39] Water molecules were located with the ARP/wARP solvent within the CCP4i GUI,[40] and verified manually. Refinement with restraints between bonded and non-crystallographic symmetry related atoms using anisotropic TLS parameters and REFMAC5[41] yielded excellent values for R_{work} and R_{free} as well as r.m.s.d. bond and angle values (Table S1†).

Scaffold 3. Trimesic acid (630.4 mg, 3.00 mmol) and EDCI (1898 mg, 9.90 mmol) were suspended in dry DCM (15 mL) under argon. After stirring for 15 min at 0 °C, Boc-DOOA (2458 mg, 9.90 mmol) was added dropwise, and the mixture was stirred overnight at RT. The resulting orange solution was washed with water (3 × 25 mL), and after separation, the organic layer was dried over anhydrous Na_2SO_4. The filtrate was concentrated to dryness and purified by flash column chromatography (DCM) to yield 1539.8 mg (1.71 mmol, 57%) of a slightly yellow oil. ^{1}H-NMR ($CDCl_3$, 600 MHz): δ [ppm] = 8.41 (s, 3 H), 7.10–7.33 (m, 3 H), 5.29 (br. s, 3 H), 3.62–3.70 (m, 24 H), 3.56 (t, J = 5.3 Hz, 6 H), 3.29 (t, J = 4.7 Hz, 6 H), 1.40 (s, 27 H). ^{13}C-NMR ($CDCl_3$, 91 MHz): δ [ppm] = 166.0, 156.2, 135.1, 128.5, 79.3, 70.3, 70.2, 69.7, 40.6, 40.1, 28.4. MS (ESI, positive): $C_{42}H_{72}N_6O_{15}$ $[M + H]^+$ calc.: 901.51, found: 901.41.

Scaffold 4. Scaffold **3** (180 mg, 0.200 mmol) was dissolved in 10 mL methanol. After cooling to 0 °C, concentrated HCl (2.2 mL, 26.6 mmol) was added dropwise. The reaction was stirred in the cold until TLC indicated full deprotection. After evaporation of the solvent, the residue was re-dissolved in methanol and stepwise neutralized to pH 7 with a saturated solution of sodium methoxide in methanol. The generated sodium chloride was filtered off and the filtrate was dried over anhydrous sodium sulfate. After evaporation, the free triamine compound was afforded quantitatively and was directly used for further reactions. ^{1}H-NMR ($CDCl_3$–CD_3OD, 600 MHz): δ [ppm] = 8.56 (s, 3 H), 3.68–3.77 (m, 12 H), 3.64 (s, 12 H), 3.38 (s, 3 H), 3.05–3.10 (m, 6 H), 2.76–3.04 (m, 6 H). ^{13}C-NMR ($CDCl_3$–CD_3OD, 151 MHz): δ [ppm] = 167.1, 134.5, 129.3, 69.9, 69.8, 69.5, 66.2, 39.7, 39.4. MS (ESI, positive): $C_{27}H_{48}N_6O_9$ $[M + H]^+$ calc.: 601.71 found: 601.60.

Scaffold 5. Scaffold **4** (240 mg, 0.400 mmol) and DIPEA (500 μL, 2.86 mmol) were dissolved in 10 mL chloroform. After pre-activation of 2-bromoacetic acid (555 mg, 4.00 mmol) with DIC (778 μL, 4.99 mmol) in chloroform (5 mL) at 0 °C for 20 min, the solution was added dropwise into the reaction mixture and stirred at RT until no educt was evident by TLC. After evaporation of the solvent the crude solid was purified *via* flash column chromatography on silica gel (DCM–methanol: 1% → 8%) yielding 50.1 mg (0.052 mmol, 13%) of a yellow solid product. ^{1}H-NMR ($CDCl_3$–CD_3OD, 600 MHz): δ [ppm] = 8.46 (s, 3 H), 4.20 (s, 9 H), 3.79 (s, 3 H), 3.59–3.70 (m, 18 H), 3.55 (t, J = 5.3 Hz, 6 H), 3.38 (t, J = 5.3 Hz, 6 H). ^{13}C-NMR ($CDCl_3$–CD_3OD, 91 MHz): δ [ppm] = 168.0, 167.5, 135.4, 129.5, 70.6, 70.6, 70.1, 69.8, 40.3, 40.2, 28.7. MS (ESI, positive): $C_{33}H_{51}Br_3N_6O_{12}$, $[M + H]^+$ calc.: 964.51 found: 964.70.

Scaffold 6. Scaffold **4** (180 mg, 0.300 mmol) and DIPEA (0.052 mL, 0.300 mmol) were dissolved in 10 mL chloroform. EDCI (230 mg, 1.199 mmol) was added. To the white suspension, 2-azidoacetic acid (182 mg, 1.798 mmol) was added dropwise and allowed to react at RT for 8 h. The reaction was then quenched with water (3 × 25 mL), the organic layer dried over anhydrous Na_2SO_4, concentrated, and the crude product purified by flash column chromatography on silica gel (DCM–methanol 1% → 5%) yielding 50.9 mg (0.06 mmol, 20%) of product. ^{1}H-NMR ($CDCl_3$–CD_3OD, 600 MHz): δ [ppm] = 8.46 (s, 3 H), 4.64 (s, 12 H), 3.89 (s, 3 H), 3.63–3.75 (m, 12 H), 3.59 (t, J = 5.5 Hz, 6 H), 3.41–3.50 (m, 6 H), 3.38 (s, 3 H). ^{13}C-NMR ($CDCl_3$–CD_3OD, 151 MHz): δ [ppm] = 167.9, 166.6, 134.6, 128.3, 69.5, 68.9, 68.7, 51.4, 39.3, 38.5, 26.2. MS (ESI, positive): $C_{33}H_{51}N_{15}O_{12}$, $[M + H]^+$ calc.: 849.87 found: 849.80.

Scaffold 7. Scaffold **4** (244 mg, 0.406 mmol) was dissolved in 10 mL chloroform. After pre-activation of bis-Boc-aminooxyacetic acid (390 mg, 1.340 mmol) with EDCI (701 mg, 3.66 mmol) in chloroform (5 mL) for 20 min at 0 °C, the resulting suspension was added dropwise to the amine. The mixture turned slowly into a colorless solution and was stirred overnight at RT. The reaction was quenched with water (30 mL). After separation, the organic layer was dried with anhydrous $MgSO_4$, filtered and evaporated until dryness. The protected scaffold was purified *via* flash column chromatography (DCM–methanol: 1% → 5%) yielding 126.5 mg (0.154 mmol, 38%) of product. The Boc groups were removed with 20% TFA in DCM (10 mL) for two hours. After evaporating the solvent, the solid was re-dissolved in DCM and evaporated three times, dried under vacuum and used without further purification. ^{1}H-NMR ($CDCl_3$–CD_3OD, 600 MHz): δ [ppm] = 8.45 (br. s, 3 H), 4.03 (br. s, 28 H), 3.66 (br. s, 24 H), 3.60 (br. s, 6 H), 3.44 (br. s, 6 H). ^{13}C-NMR ($CDCl_3$–CD_3OD, 151 MHz): δ [ppm] = 167.2, 135.1, 129.1, 70.3, 70.2, 69.8, 69.7, 69.6, 69.5, 40.1, 40.1, 38.8. MS (ESI, positive): $C_{33}H_{57}N_9O_{15}$, $[M + H]^+$ calc.: 820.86 found: 820.70.

Trivalent peptide 12. Solutions of peptide **9** (12 mM) and scaffold **5** (4 mM, 100 μL each, both in ACN–water (1 : 1)) were mixed with 200 μL 0.1 M carbonate buffer pH 9.6, resulting in a final concentration of 1 mM of peptide **9**. After an overnight reaction, the product was analyzed by LC-MS, lyophilized, purified by preparative HPLC, and analyzed by LC-MS.

Trivalent peptides 13, 18 and 19. Solutions of peptides **10**, **16** and **17**, respectively (100 μL, 12 mM in isopropanol–water (1 : 1)), were mixed with 100 μL of 4 mM scaffold **6** solution, 100 μL of 24 mM $CuSO_4$ in isopropanol–water (1 : 1), as well as with 100 μL of 72 mM sodium ascorbate in isopropanol–water (1 : 1), resulting in a final concentration of 1 mM of peptides. Isopropanol can be replaced with DMF. After an overnight reaction, the product was analyzed by LC-MS, lyophilized, purified by preparative HPLC, and analyzed by LC-MS and high resolution ESI mass spectrometry (**18** and **19**).

Trivalent peptide 14. Solutions of peptide **11** (12 mM) and scaffold **8** (4 mM, 100 μL each, both in ACN–water (1 : 1)) were mixed with 200 μL of 0.1 M citrate buffer pH 2.5, resulting in a final concentration of 1 mM of peptide **14**. After an overnight

reaction, the product was analyzed by LC-MS, lyophilized, purified by preparative HPLC, and analyzed by LC-MS.

Conclusions

In conclusion, we have generated three differently functionalized C_3-symmetric scaffolds based on trimesic acid for the trivalent presentation of biomolecules. The utility of these versatile scaffolds for trimerization reactions was demonstrated using appropriately functionalized peptides in conjunction with three different ligation strategies, *i.e.* thioether formation, click chemistry and oxime ligation, respectively. Kinetic analysis of each ligation reaction demonstrated that all three reactions are powerful tools for the synthesis of trivalent peptides. Depending on the desired flexibility of the trivalent molecules, the length and flexibility of the spacer can be varied using other diamines. It should also be noted that the utility of these scaffolds is not limited to the three ligation reactions presented here, but could readily be extended to include other ligation reactions, such as Staudinger ligation[42] and native chemical ligation,[43] simply by reacting the scaffold amino groups with appropriate chemical moieties. Furthermore, covalent attachment of alkyne-modified foldon peptides to the triazido scaffold using the click reaction distinctly enhanced the stability of the foldon trimer, while maintaining its correct fold. This illustrates an alternative application of multivalent peptide presentation, in which folded, non-covalent peptide and protein oligomers are thermodynamically stabilized by covalently linking the monomers to an appropriate multivalent scaffold.

Abbreviations

ACN	Acetonitrile
Boc	*t*-Butyloxycarbonyl
DCM	Dichloromethane
DIC	*N*,*N*′-Diisopropylcarbodiimide
DIPEA	*N*,*N*-Diisopropylamine
DOOA	3,6-Dioxaoctane-1,8-diamine
EDCI	1-Ethyl-3-(3-dimethylaminopropyl)carbodiimide
EDT	1,2-Ethanedithiol
Fmoc	9-Fluorenylmethoxycarbonyl
HOBt	1-Hydroxybenzotriazole
TFA	Trifluoroacetic acid.

Acknowledgements

This work was supported by SFB 796 (Project A5) from the German Research Foundation (DFG). We thank Astrid König for excellent technical assistance (crystallization experiments), Frank Hampel for high resolution ESI mass spectra and Thomas Kiefhaber for valuable advice regarding thermal unfolding transition measurements. The coordinates and structure factors of the two covalent conjugates **18** and **19**, have been deposited in the Protein Databank (PDB accession codes 4NCV and 4NCW).

Notes and references

1 C. Fasting, C. A. Schalley, M. Weber, O. Seitz, S. Hecht, B. Koksch, J. Dernedde, C. Graf, E.-W. Knapp and R. Haag, *Angew. Chem., Int. Ed.*, 2012, **51**, 10472–10498.
2 B. Stephens and T. M. Handel, in *Progress in Molecular Biology and Translational Science*, ed. K. Terry, Academic Press, 2013, vol. 115, pp. 375–420.
3 M. G. Tansey and D. E. Szymkowski, *Drug Discovery Today*, 2009, **14**, 1082–1088.
4 J. Liu, A. Bartesaghi, M. J. Borgnia, G. Sapiro and S. Subramaniam, *Nature*, 2008, **455**, 109–113.
5 P. Zhu, J. Liu, J. Bess Jr., E. Chertova, J. D. Lifson, H. Grise, G. A. Ofek, K. A. Taylor and K. H. Roux, *Nature*, 2006, **441**, 847–852.
6 B. J. Doranz, S. S. W. Baik and R. W. Doms, *J. Virol.*, 1999, **73**, 10346–10358.
7 J. Eichler, *Curr. Opin. Chem. Biol.*, 2008, **12**, 707–713.
8 F. M. Brunel and P. E. Dawson, *Chem. Commun.*, 2005, 2552–2554.
9 J. E. Moses and A. D. Moorhouse, *Chem. Soc. Rev.*, 2007, **36**, 1249–1262.
10 C. P. Hackenberger and D. Schwarzer, *Angew. Chem., Int. Ed.*, 2008, **47**, 10030–10074.
11 D. M. Eckert and P. S. Kim, *Proc. Natl. Acad. Sci. U. S. A.*, 2001, **98**, 11187–11192.
12 E. Bianchi, M. Finotto, P. Ingallinella, R. Hrin, A. V. Carella, X. S. Hou, W. A. Schleif, M. D. Miller, R. Geleziunas and A. Pessi, *Proc. Natl. Acad. Sci. U. S. A.*, 2005, **102**, 12903–12908.
13 V. V. Mesyanzhinov, in *Advances in Virus Research*, Academic Press, Editon edn, 2004, vol. 63, pp. 287–352.
14 Y. Tao, S. V. Strelkov, V. V. Mesyanzhinov and M. G. Rossmann, *Structure*, 1997, **5**, 789–798.
15 S. Güthe, L. Kapinos, A. Möglich, S. Meier, S. Grzesiek and T. Kiefhaber, *J. Mol. Biol.*, 2004, **337**, 905–915.
16 Z. Qi, C. Pan, H. Lu, Y. Shui, L. Li, X. Li, X. Xu, S. Liu and S. Jiang, *Biochem. Biophys. Res. Commun.*, 2010, **398**, 506–512.
17 T. Ito, K. Iwamoto, I. Tsuji, H. Tsubouchi, H. Omae, T. Sato, H. Ohba, T. Kurokawa, Y. Taniyama and Y. Shintani, *Appl. Microbiol. Biotechnol.*, 2011, **90**, 1691–1699.
18 L. Du, V. H.-C. Leung, X. Zhang, J. Zhou, M. Chen, W. He, H.-Y. Zhang, C. C. S. Chan, V. K.-M. Poon, G. Zhao, S. Sun, L. Cai, Y. Zhou, B.-J. Zheng and S. Jiang, *PLoS One*, 2011, **6**, e16555.
19 D. Seebach, G. F. Herrmann, U. D. Lengweiler, B. M. Bachmann and W. Amrein, *Angew. Chem., Int. Ed. Engl.*, 1996, **35**, 2795–2797.

20 Y. Nishida, T. Tsurumi, K. Sasaki, K. Watanabe, H. Dohi and K. Kobayashi, *Org. Lett.*, 2003, **5**, 3775–3778.
21 H. Kubas, M. Schafer, U. Bauder-Wust, M. Eder, D. Oltmanns, U. Haberkorn, W. Mier and M. Eisenhut, *Nucl. Med. Biol.*, 2010, **37**, 885–891.
22 H. Li, Y. Guan, A. Szczepanska, A. J. Moreno-Vargas, A. T. Carmona, I. Robina, G. K. Lewis and L. X. Wang, *Bioorg. Med. Chem.*, 2007, **15**, 4220–4228.
23 A. Torres, C. Mas-Moruno, E. Perez-Paya, F. Albericio and M. Royo, *Bioconjugate Chem.*, 2011, **22**, 2172–2178.
24 E.-M. Kim, M.-H. Joung, C.-M. Lee, H.-J. Jeong, S. T. Lim, M.-H. Sohn and D. W. Kim, *Bioorg. Med. Chem. Lett.*, 2010, **20**, 4240–4243.
25 D. J. Hlasta and J. H. Ackerman, *J. Org. Chem.*, 1994, **59**, 6184–6189.
26 J. Eichler and R. A. Houghten, *Biochemistry*, 1993, **32**, 11035–11041.
27 H. Lindley, *Biochem. J.*, 1960, **74**, 577–584.
28 M. Monso, W. Kowalczyk, D. Andreu and B. G. de la Torre, *Org. Biomol. Chem.*, 2012, **10**, 3116–3121.
29 H. C. Kolb, M. G. Finn and K. B. Sharpless, *Angew. Chem., Int. Ed.*, 2001, **40**, 2004–2021.
30 A. Brik, J. Alexandratos, Y. C. Lin, J. H. Elder, A. J. Olson, A. Wlodawer, D. S. Goodsell and C. H. Wong, *ChemBioChem: a Eur. J. Chem. Biol.*, 2005, **6**, 1167–1169.
31 S. Punna, J. Kuzelka, Q. Wang and M. G. Finn, *Angew. Chem., Int. Ed.*, 2005, **44**, 2215–2220.
32 Y. Angell and K. Burgess, *J. Org. Chem.*, 2005, **70**, 9595–9598.
33 P. Marceau, C. Bure and A. F. Delmas, *Bioorg. Med. Chem. Lett.*, 2005, **15**, 5442–5445.
34 A. Dirksen, T. M. Hackeng and P. E. Dawson, *Angew. Chem., Int. Ed.*, 2006, **45**, 7581–7584.
35 J. Habazettl, A. Reiner and T. Kiefhaber, *J. Mol. Biol.*, 2009, **389**, 103–114.
36 W. Kabsch, *J. Appl. Crystallogr.*, 1993, **26**, 795–800.
37 A. J. McCoy, R. W. Grosse-Kunstleve, P. D. Adams, M. D. Winn, L. C. Storoni and R. J. Read, *J. Appl. Crystallogr.*, 2007, **40**, 658–674.
38 D. Turk, *Acta Crystallogr.*, 2013, **D69**, 1342–1357.
39 G. N. Murshudov, A. A. Vagin and E. J. Dodson, *Acta Crystallogr., Sect. D: Biol. Crystallogr.*, 1997, **53**, 240–255.
40 A. Perrakis, R. Morris and V. Lamzin, *Nat. Struct. Biol.*, 1999, **6**, 458–463.
41 A. A. Vagin, R. A. Steiner, A. A. Lebedev, L. Potterton, S. McNicholas, F. Long and G. N. Murshudov, *Acta Crystallogr., Sect. D: Biol. Crystallogr.*, 2004, **60**, 2184–2195.
42 M. Köhn and R. Breinbauer, *Angew. Chem., Int. Ed.*, 2004, **43**, 3106–3116.
43 C. Haase and O. Seitz, *Angew. Chem., Int. Ed.*, 2008, **47**, 1553–1556.

